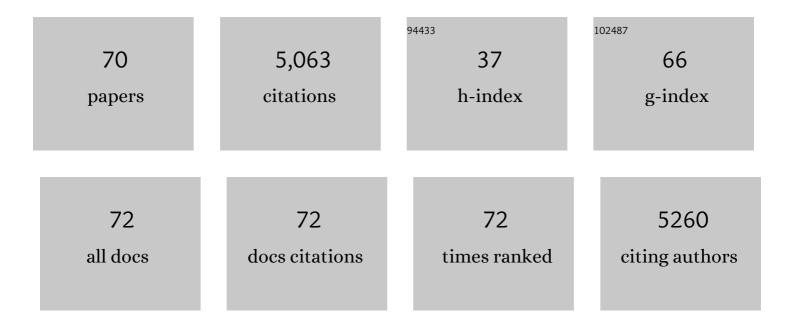
List of Publications by Year in descending order

Source: https://exaly.com/author-pdf/8632366/publications.pdf Version: 2024-02-01



GUANNA LI

#	Article	IF	CITATIONS
1	A highly selective and stable ZnO-ZrO ₂ solid solution catalyst for CO ₂ hydrogenation to methanol. Science Advances, 2017, 3, e1701290.	10.3	683
2	Single-site trinuclear copper oxygen clusters in mordenite for selective conversion of methane to methanol. Nature Communications, 2015, 6, 7546.	12.8	623
3	Intrinsic Facetâ€Dependent Reactivity of Wellâ€Defined BiOBr Nanosheets on Photocatalytic Water Splitting. Angewandte Chemie - International Edition, 2020, 59, 6590-6595.	13.8	231
4	Stability and reactivity of copper oxo-clusters in ZSM-5 zeolite for selective methane oxidation to methanol. Journal of Catalysis, 2016, 338, 305-312.	6.2	217
5	Isolated Fe Sites in Metal Organic Frameworks Catalyze the Direct Conversion of Methane to Methanol. ACS Catalysis, 2018, 8, 5542-5548.	11.2	200
6	Phosphorus Induced Electron Localization of Single Iron Sites for Boosted CO ₂ Electroreduction Reaction. Angewandte Chemie - International Edition, 2021, 60, 23614-23618.	13.8	197
7	Stable Mo/HZSM-5 methane dehydroaromatization catalysts optimized for high-temperature calcination-regeneration. Journal of Catalysis, 2017, 346, 125-133.	6.2	147
8	A Thorough Investigation of the Active Titanium Species in TSâ€I Zeolite by In Situ UV Resonance Raman Spectroscopy. Chemistry - A European Journal, 2012, 18, 13854-13860.	3.3	137
9	High-Performance M _a ZrO _{<i>x</i>} (M _a = Cd, Ga) Solid-Solution Catalysts for CO ₂ Hydrogenation to Methanol. ACS Catalysis, 2019, 9, 10253-10259.	11.2	137
10	Synergy between Lewis acid sites and hydroxyl groups for the isomerization of glucose to fructose over Sn-containing zeolites: a theoretical perspective. Catalysis Science and Technology, 2014, 4, 2241-2250.	4.1	117
11	Catalytic Hydrogenation of CO ₂ to Formates by a Lutidine-Derived Ru–CNC Pincer Complex: Theoretical Insight into the Unrealized Potential. ACS Catalysis, 2015, 5, 1145-1154.	11.2	109
12	Synthesis of Snâ€Beta with Exclusive and High Framework Sn Content. ChemCatChem, 2015, 7, 1152-1160.	3.7	105
13	Understanding the Effect of Crystalline Structural Transformation for Leadâ€Free Inorganic Halide Perovskites. Advanced Materials, 2020, 32, e2002137.	21.0	101
14	Mechanistic Complexity of Methane Oxidation with H ₂ O ₂ by Single-Site Fe/ZSM-5 Catalyst. ACS Catalysis, 2018, 8, 7961-7972.	11.2	98
15	The Nature and Catalytic Function of Cation Sites in Zeolites: a Computational Perspective. ChemCatChem, 2019, 11, 134-156.	3.7	96
16	Lateral Adsorbate Interactions Inhibit HCOO ^{â^'} while Promoting CO Selectivity for CO ₂ Electrocatalysis on Silver. Angewandte Chemie - International Edition, 2019, 58, 1345-1349.	13.8	93
17	Nature and Catalytic Role of Extraframework Aluminum in Faujasite Zeolite: A Theoretical Perspective. ACS Catalysis, 2015, 5, 7024-7033.	11.2	92
18	Engineering the Protein Corona Structure on Gold Nanoclusters Enables Redâ€Shifted Emissions in the Second Nearâ€infrared Window for Gastrointestinal Imaging. Angewandte Chemie - International Edition, 2020, 59, 22431-22435.	13.8	78

#	Article	IF	CITATIONS
19	In Situ UV Raman Spectroscopic Studies on the Synthesis Mechanism of Zeolite X. Chemistry - A European Journal, 2008, 14, 5125-5129.	3.3	75
20	Stability of Extraframework Iron-Containing Complexes in ZSM-5 Zeolite. Journal of Physical Chemistry C, 2013, 117, 413-426.	3.1	75
21	Electronic Structure of the [Cu ₃ (μ-O) ₃] ²⁺ Cluster in Mordenite Zeolite and Its Effects on the Methane to Methanol Oxidation. Journal of Physical Chemistry C, 2017, 121, 22295-22302.	3.1	74
22	Relationship between acidity and catalytic reactivity of faujasite zeolite: A periodic DFT study. Journal of Catalysis, 2016, 344, 570-577.	6.2	72
23	Stability and reactivity of active sites for direct benzene oxidation to phenol in Fe/ZSM-5: A comprehensive periodic DFT study. Journal of Catalysis, 2011, 284, 194-206.	6.2	69
24	Unraveling reaction networks behind the catalytic oxidation of methane with H ₂ O ₂ over a mixed-metal MIL-53(Al,Fe) MOF catalyst. Chemical Science, 2018, 9, 6765-6773.	7.4	67
25	Dehydration of Glucose to 5â€Hydroxymethylfurfural Using Nbâ€doped Tungstite. ChemSusChem, 2016, 9, 2421-2429.	6.8	64
26	Formation of Active Cu-oxo Clusters for Methane Oxidation in Cu-Exchanged Mordenite. Journal of Physical Chemistry C, 2019, 123, 8759-8769.	3.1	60
27	Finding the "Missing Components―during the Synthesis of TS-1 Zeolite by UV Resonance Raman Spectroscopy. Journal of Physical Chemistry C, 2013, 117, 2844-2848.	3.1	56
28	Structure and Reactivity of the Mo/ZSM-5 Dehydroaromatization Catalyst: An Operando Computational Study. ACS Catalysis, 2019, 9, 8731-8737.	11.2	52
29	Activity Descriptors Derived from Comparison of Mo and Fe as Active Metal for Methane Conversion to Aromatics. Journal of the American Chemical Society, 2019, 141, 18814-18824.	13.7	52
30	Engineering the Protein Corona Structure on Gold Nanoclusters Enables Redâ€Shifted Emissions in the Second Nearâ€infrared Window for Gastrointestinal Imaging. Angewandte Chemie, 2020, 132, 22617-22621.	2.0	52
31	Shape-Controlled Copper Selenide Nanocubes Synthesized by an Electrochemical Crystallization Method. Journal of Physical Chemistry C, 2009, 113, 10833-10837.	3.1	48
32	Relevance of the Mo-precursor state in H-ZSM-5 for methane dehydroaromatization. Catalysis Science and Technology, 2018, 8, 916-922.	4.1	47
33	Intrinsic Facetâ€Dependent Reactivity of Wellâ€Defined BiOBr Nanosheets on Photocatalytic Water Splitting. Angewandte Chemie, 2020, 132, 6652-6657.	2.0	46
34	A Periodic DFT Study of Glucose to Fructose Isomerization on Tungstite (WO ₃ A·H ₂ O): Influence of Group IV–VI Dopants and Cooperativity with Hydroxyl Groups. ACS Catalysis, 2016, 6, 4162-4169.	11.2	45
35	Breaking Linear Scaling Relationships with Secondary Interactions in Confined Space: A Case Study of Methane Oxidation by Fe/ZSM-5 Zeolite. ACS Catalysis, 2019, 9, 9276-9284.	11.2	44
36	Catalytic properties of extraframework iron-containing species in ZSM-5 for N2O decomposition. Journal of Catalysis, 2013, 308, 386-397.	6.2	43

#	Article	IF	CITATIONS
37	Controlled Growth of Monodisperse Ferrite Octahedral Nanocrystals for Biomass-Derived Catalytic Applications. ACS Catalysis, 2017, 7, 2948-2955.	11.2	40
38	A site-sensitive quasi-in situ strategy to characterize Mo/HZSM-5 during activation. Journal of Catalysis, 2019, 370, 321-331.	6.2	40
39	Divalent Ion Selectivity in Capacitive Deionization with Vanadium Hexacyanoferrate: Experiments and Quantumâ€Chemical Computations. Advanced Functional Materials, 2021, 31, 2105203.	14.9	38
40	Competitive Adsorption of Substrate and Solvent in Snâ€Beta Zeolite During Sugar Isomerization. ChemSusChem, 2016, 9, 3145-3149.	6.8	36
41	Structure-activity relationships in metal organic framework derived mesoporous nitrogen-doped carbon containing atomically dispersed iron sites for CO2 electrochemical reduction. Journal of Catalysis, 2019, 378, 320-330.	6.2	36
42	Interfacial Modulation with Aluminum Oxide for Efficient Plasmonâ€Induced Water Oxidation. Advanced Functional Materials, 2021, 31, 2005688.	14.9	33
43	Effect of the Nature and Location of Copper Species on the Catalytic Nitric Oxide Selective Catalytic Reduction Performance of the Copper/SSZâ€13 Zeolite. ChemCatChem, 2014, 6, 634-639.	3.7	30
44	A Density Functional Theory Study of the Mechanism of Direct Glucose Dehydration to 5â€Hydroxymethylfurfural on Anatase Titania. ChemCatChem, 2018, 10, 4084-4089.	3.7	27
45	Lateral Adsorbate Interactions Inhibit HCOO ^{â^'} while Promoting CO Selectivity for CO ₂ Electrocatalysis on Silver. Angewandte Chemie, 2019, 131, 1359-1363.	2.0	25
46	Antibiotic-Like Activity of Atomic Layer Boron Nitride for Combating Resistant Bacteria. ACS Nano, 2022, 16, 7674-7688.	14.6	25
47	Highly dispersed Cd cluster supported on TiO2 as an efficient catalyst for CO2 hydrogenation to methanol. Chinese Journal of Catalysis, 2022, 43, 761-770.	14.0	24
48	Phosphorus Induced Electron Localization of Single Iron Sites for Boosted CO ₂ Electroreduction Reaction. Angewandte Chemie, 2021, 133, 23806-23810.	2.0	22
49	ldentification of Fe2(μ-O) and Fe2(μ-O)2 sites in Fe/ZSM-35 by in situ resonance Raman spectroscopy. Journal of Catalysis, 2013, 301, 77-82.	6.2	21
50	Property–Activity Relations for Methane Activation by Dualâ€Metal Cu–Oxo Trimers in ZSMâ€5 Zeolite. Small Methods, 2018, 2, 1800266.	8.6	21
51	Zinc and cadmium coordination polymers assembled with 2,2′-bipyridine and bithiophenedicarboxylic acid: Effect of metal ions on the conformation of ligand. Inorganica Chimica Acta, 2012, 383, 185-189.	2.4	18
52	Gold and Silver-Catalyzed Reductive Amination of Aromatic Carboxylic Acids to Benzylic Amines. ACS Catalysis, 2021, 11, 7672-7684.	11.2	18
53	Chirality transition in the epoxidation of (â^')-α-pinene and successive hydrolysis studied by Raman optical activity and DFT. Physical Chemistry Chemical Physics, 2010, 12, 3005.	2.8	14
54	pH-Dependent Chirality of <scp>l</scp> -Proline Studied by Raman Optical Activity and Density Functional Theory Calculation. Journal of Physical Chemistry A, 2011, 115, 1340-1349.	2.5	11

#	Article	IF	CITATIONS
55	Enhanced surface area and reduced pore collapse of methylated, imine-linked covalent organic frameworks. Nanoscale, 2021, 13, 19446-19452.	5.6	10
56	Hydrogen bonding in homochiral dimers of hydroxyesters studied by Raman optical activity spectroscopy. Journal of Raman Spectroscopy, 2012, 43, 503-513.	2.5	9
57	"Extracting―the Key Fragment in ETSâ€10 Crystallization and Its Application in AMâ€6 Assembly. Chemistry A European Journal, 2012, 18, 12078-12084.	- 3.3	8
58	Single-Atom Pt ⁺ Derived from the Laser Dissociation of a Platinum Cluster: Insights into Nonoxidative Alkane Conversion. Journal of Physical Chemistry Letters, 2020, 11, 5987-5991.	4.6	8
59	Alizarin Grafting onto Ultrasmall ZnO Nanoparticles: Mode of Binding, Stability, and Colorant Studies. Langmuir, 2021, 37, 1446-1455.	3.5	8
60	Unraveling the Nature of Extraframework Catalytic Ensembles in Zeolites: Flexibility and Dynamics of the Copper-Oxo Trimers in Mordenite. Journal of Physical Chemistry Letters, 2021, 12, 10906-10913.	4.6	8
61	Solvent-Assisted Ketone Reduction by a Homogeneous Mn Catalyst. Organometallics, 2022, 41, 1829-1835.	2.3	8
62	Alkali-hydrolysis of D-glucono-delta-lactone studied by chiral Raman and circular dichroism spectroscopies. Science in China Series B: Chemistry, 2009, 52, 552-558.	0.8	6
63	Effect of Substituted Groups on the Electronic Circular Dichroism of Aldols: A Combined Experimental and Time-Dependent DFT Study. Journal of Physical Chemistry C, 2011, 115, 972-981.	3.1	5
64	Ground-state properties of the narrowest zigzag graphene nanoribbon from quantum Monte Carlo and comparison with density functional theory. Journal of Chemical Physics, 2022, 156, 084112.	3.0	4
65	Lewis Acid Catalysis by Zeolites * *These authors contributed equally , 2018, , 229-263.		3
66	Mechanistic investigation of benzene esterification by K2CO3/TiO2: the catalytic role of the multifunctional interface. Chemical Communications, 2021, 57, 7890-7893.	4.1	2
67	Chiral Sulfur Compounds Studied by Raman Optical Activity: <i>tert</i> â€Butanesulfinamide and its Precursor <i>tert</i> â€Butyl <i>tert</i> â€Butanethiosulfinate. Chirality, 2012, 24, 731-740.	2.6	1
68	Metal Containing Nanoclusters in Zeolites. , 2021, , .		1
69	CO 2 Hydrogenation to Methanol over Cd 4 /TiO 2 Catalyst: Insight into Multifunctional Interface. ChemCatChem, 0, , .	3.7	1
70	Rücktitelbild: Lateral Adsorbate Interactions Inhibit HCOO ^{â^'} while Promoting CO Selectivity for CO ₂ Electrocatalysis on Silver (Angew. Chem. 5/2019). Angewandte Chemie, 2019, 131, 1534-1534.	2.0	0